Penerbit Akademia Baru

Journal of Advanced Research in Fluid Mechanics and Thermal Sciences

Journal homepage: www.akademiabaru.com/arfmts.html
ISSN: 2289-7879

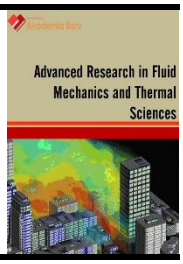


# Heat and Mass Transfer Effect on Non-Newtonian Fluid Flow in a Non-uniform Vertical Tube with Peristalsis

Open Access

Hesham Mohamed Mansour[1], Mohamed Y. Abou-zeid[2,*]

[1] Department of Physics, Faculty of Science, Cairo University, Giza,12613, Egypt
[2] Department of Mathematics, Faculty of Education, Ain Shams University, Heliopolis, Cairo, 11757, Egypt

**ARTICLE INFO**

***Article history:***
Received 24 April 2019
Received in revised form 24 July 2019
Accepted 27 August 2019
Available online 19 September 2019

***Keywords:***
Non-Newtonian fluid; heat and mass transfer; peristaltic motion

**ABSTRACT**

This article deals with the influence of heat and mass transfer on peristaltic flow of non-Newtonian Williamson fluid in the gap between concentric tubes. A perturbation solution, under the assumptions of long wavelength and low Reynolds number is obtained which satisfies the momentum, energy and concentration equations for the case of small porosity parameter and Weisseing number. Numerical results for the behaviors of the velocity, temperature and concentration as well as the skin friction, Nusselt number and Sherwood number with other physical parameters are displayed and discussed in detail. The obtained results point to that the temperature increases with the increase each of Eckert number Ec and Weisseing number, We. While, an opposite behavior for the concentration compared to temperature behavior is found. Morever, The axial velocity decreases with the increase each of Sc and Sr, whereas it decreases as Ec, GT and GC increase.



## 1. Introduction

Peristalsis is an important mechanism for mixing and transporting fluids, which is generated by a progressive wave of contraction or expansion moving on the wall of the tube. Physiological fluids in animal and human bodies are, in general, pumped by the continuous periodic muscular oscillations of the ducts. These oscillations are presumed to be caused by the progressive transverse contraction waves that propagate along the walls of the ducts. Peristaltic flow occurs widely in the functioning of the ureter, food mixing and chime movement in the intestine, movement of eggs in the fallopian tube, the transport of the spermatozoa in cervical canal, transport of bile in the bile duct, transport of cilia, and circulation of blood in small blood vessels. Peristaltic flows have attracted several researchers because of wide applications in physiology and industry.

The theoretical work on peristaltic transport with sinusoidal transverse wave of small amplitude is primarily investigated by Fung and Yih [1]. Burns and Parkes [2] studied the peristaltic motion of a viscous fluid through a pipe and a channel by considering sinusoidal variation at the walls. Abd El-

* *Corresponding author.*
*E-mail address: master_math2003@yahoo.com (Mohamed Y. Abou-zeid)*

Naby and El-Misiery [3] picked up peristaltic pumping of a Carreau fluid in presence of an endoscope. Recently a study of ureteral peristalsis in cylindrical tube through porous medium has been discussed by Rathod *et al.,* [4]. A variety of analysis have been presented on the peristaltic problems keeping different flow geometries and fluid models [5-11].

In the studies mentioned above, the peristaltic problems in the absence of heat and mass transfer are considered. Only limited studies have been made to examine the effects of heat and mass transfer on the peristaltic flow problems [12-21].

Flow through a porous medium has several practical applications especially in geophysical fluid dynamics. Examples of natural porous media are beach sand, sandstone, limestone, the human lung, bile duct, gall bladder with stones in small blood vessels. The first study of peristaltic flow through a porous medium is presented by Afifi [22]. El-Shehawey *et al.,* [23] studied the peristaltic flow of a generalized Newtonian fluid thorough a porous medium. The effects of chemical reaction on the interaction among peristalsis, heat, and mass transfer for the motion of a non-Newtonian Jeffrey fluid embedded in a vertical porous medium in two-dimensional tubes by El-Sayed *et al.,* [24]. Hayat *et al.,* [25] studied the effect of heat transfer on the peristaltic flow of an electrically conducting fluid in a porous space.

In the previous works they studied the peristaltic motion alone or with heat and mass transfer, but they did not study the effect of the porous media in the energy equation with the existence of heat convection. This is what we will show in the next sections. In this article, a mathematical model is presented to study the effects of the interaction among peristalsis, heat, and mass transfer for the motion of a non-Newtonian Williamson fluid embedded in a porous medium between two-dimensional vertical tubes. The outer tube is non-uniform and has a sinusoidal wave traveling down its wall, and the inner one is a rigid, and uniform tube. Blood flow through arterial catheterization is considered as a model of peristaltic flow of non-Newtonian fluid. The momentum, energy, and mass equations have been linearized under long-wavelength and low Reynolds number assumptions. Analytical solutions for the velocity, temperature and concentration have been obtained. The influence of various pertinent parameters on the velocity, temperature, concentration, skin-friction, Nusselt number and Sherwood number are discussed in detail through graphs. This study may have application in many clinical applications such as the endoscope problem.

## 2. Formulation of The Problem

Consider the flow with heat and mass transfer of an incompressible non-Newtonian fluid obeying Williamson model through a porous medium in the gap between two coaxial vertical tubes. The inner tube is rigid and uniform, while the outer tube has a sinusoidal wave traveling down its wall. We choose a rectangular coordinate system for the tubes with y along the center line of the inner and the outer tubes, x is the radial distance measured, the inner tube is at $x = x_1$ and kept at a temperature Ti and concentration $C_i$, and the outer tube is at $x = x_2$ and kept at a temperature To and concentration Co. The geometry of the wall surfaces is described in Figure 1, the equations for the radii are

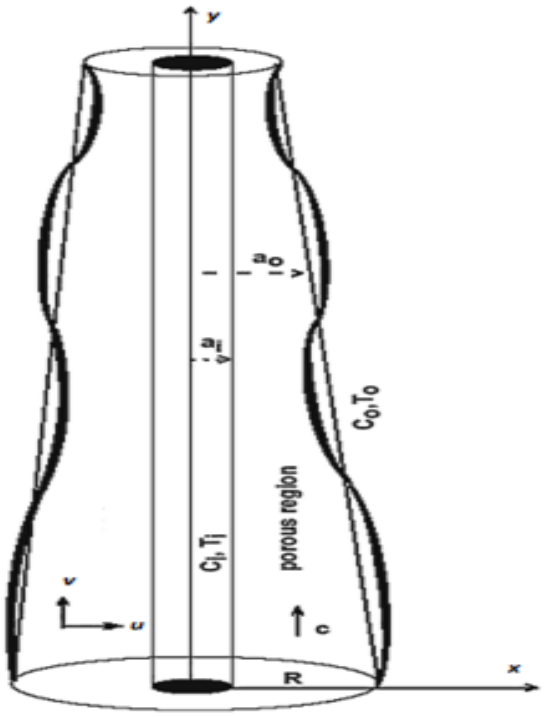


**Fig. 1.** The geometry of the wall surfaces

$$x_1 = a_i\,, \tag{1}$$

$$x_2 = a_o + b\sin\frac{2\pi}{\lambda}(y - ct)\,, \tag{2}$$

where $a_i$ signifies the radius of the inner tube, $a_o$ indicates the radius of the outer tube at the inlet, b is the wave amplitude, $\lambda$ is the wavelength, c is the propagation velocity along $y$ direction, and $t$ is the time. The radius of the tapered tube is given by El-Sayed *et al.,* [24]

$$a_o = R - y\tan\psi\,, \tag{3}$$

where R is the radius at y = 0, $\psi$ is the angle of taper which is considered as a constant. The governing continuity, momentum, temperature, and concentration equations for this problem can be written as

$$\frac{\partial u}{\partial x} + \frac{\partial v}{\partial y} = 0\,, \tag{4}$$

$$\rho\left(\frac{\partial u}{\partial t} + u\frac{\partial u}{\partial x} + v\frac{\partial u}{\partial y}\right) = -\frac{\partial P}{\partial x} + \left(\frac{\partial \tau_{xx}}{\partial x} + \frac{\partial \tau_{xy}}{\partial y}\right) - \frac{\mu}{k_p}u\,, \tag{5}$$

$$\rho\left(\frac{\partial v}{\partial t} + u\frac{\partial v}{\partial x} + v\frac{\partial v}{\partial y}\right) = -\frac{\partial P}{\partial y} + \left(\frac{\partial \tau_{yx}}{\partial x} + \frac{\partial \tau_{yy}}{\partial y}\right) + \rho g\beta\,(T - \overline{T}) + \rho g\beta^*\,(C - \overline{C}) - \frac{\mu}{k_p}v\,, \tag{6}$$

$$\rho c_p\left(\frac{\partial T}{\partial t}+u\frac{\partial T}{\partial x}+v\frac{\partial T}{\partial y}\right)=k\nabla^2 T+\frac{\mu}{k_p}(u+v)\left|\underline{V}\right|, \tag{7}$$

$$\frac{\partial C}{\partial t}+u\frac{\partial C}{\partial x}+v\frac{\partial C}{\partial y}=D\nabla^2 C+\frac{Dk_T}{\overline{T}}\nabla^2 T\,. \tag{8}$$

where $\left|\underline{V}\right|=\sqrt{u^2+v^2}$ , u and v are the velocities in the x and y directions, respectively, T is the temperature, C is the concentration, $\rho$ is the fluid density, P is the pressure, $\mu$ is the dynamic viscosity, kp is the permeability of porous medium, g is the acceleration due to gravity, $\beta$ is the volumetric expansion coefficient, $\beta^*$ is the coefficient of expansion with concentration, $\overline{T}$ is the mean of Ti and To, $\overline{C}$ is the mean of Ci and Co , k is the thermal conductivity, cp is the specific heat at constant pressure, D is the mass diffusivity, and kT is the thermal diffusion ratio.

Equations for an incompressible Williamson fluid are

$$\tau_{ij}=\mu\left(1+We\,\overline{\gamma}\right)e_{ij}\,, \tag{9}$$

Here $\overline{\gamma}=\sqrt{e_{ij}e_{ij}}$, where $e_{ij}$ is the (i,j) component of the deformation rate and $We$ is Weisseing number. For ordinary Newtonian fluid ($We=0$).

The boundary conditions for this system are given by

$$u=0\,,\quad v=0\,,\quad T=T_i\quad,\quad C=C_i\qquad at\qquad x=x_1\,. \tag{10}$$

$$u=\frac{\partial x_2}{\partial t}\quad,\quad v=0\,,\quad T=T_o\quad,\quad C=C_o\qquad at\qquad x=x_2\,. \tag{11}$$

The appropriate non-dimensional variables for the flow are defined as

$$\begin{aligned} &x^*=\frac{x}{R}\,,\quad y^*=\frac{y}{\lambda}\,,\quad u^*=\frac{\lambda}{cR}u\,,\quad v^*=\frac{v}{c}\,,\quad P^*=\frac{R^2}{\lambda c\mu}P\,,\quad T^*=\frac{T-\overline{T}}{T_o-\overline{T}}\,,\\ &C^*=\frac{C-\overline{C}}{C_o-\overline{C}}\,,\quad t^*=\frac{c}{\lambda}t\,,\quad \tau^*=\frac{R}{\mu c}\tau\,,\quad x_1^{\,*}=\frac{x_1}{R}\,,\quad x_2^{\,*}=\frac{x_2}{R}\,,\quad \delta=\frac{R}{\lambda} \end{aligned}\,. \tag{12}$$

In terms of these variables, after applying the long wavelength approximation [24], and dropping the star mark for simplicity, Eq. (4)-(8) become

$$\frac{\partial u}{\partial x}+\frac{\partial v}{\partial y}=0\,, \tag{13}$$

$$\frac{\partial P}{\partial x}=0\,, \tag{14}$$

$$\frac{\partial P}{\partial y}=\frac{\partial}{\partial x}\left[\left(1+We\left(\frac{\partial v}{\partial x}\right)^{2}\right)\frac{\partial v}{\partial x}\right]+G_T\,T+G_C\,C-\varepsilon^2 v\,, \tag{15}$$

$$\frac{\partial^2 T}{\partial x^2}=\varepsilon^2 Ec\,v^2\,, \tag{16}$$

$$\frac{\partial^2 C}{\partial x^2}=-Sc\,Sr\frac{\partial^2 T}{\partial x^2}\,, \tag{17}$$

Here, $\varepsilon^2=\frac{R^2}{k_p}$ is the porous parameter, $\nu=\frac{\mu}{\rho}$ is the kinematic viscosity, $G_T=\frac{g\beta(T_o-\bar{T})R^2}{\nu c}$ is Gasthof number, $G_C=\frac{g\beta^*(C_o-\bar{C})R^2}{\nu c}$ is the modified Grashof number, $Ec=\frac{\mu c^2}{k_p(T_o-\bar{T})}$ is Eckert number, $Sc=\frac{\nu}{D}$ is Schmidt number and $Sr=\frac{D\,k_T(T_o-\bar{T})}{\nu\bar{T}(C_o-\bar{C})}$ is Soret number.

Thus, the boundary conditions (10) and (11) in their dimensionless form read

$$u=0\,,\quad v=0\,,\quad T=n\,,\quad C=m\qquad at\qquad x=x_1\,. \tag{18}$$

$$u=\frac{\partial x_2}{\partial t}\,,\quad v=0\,,\quad T=1\,,\quad C=1\qquad at\qquad x=x_2\,, \tag{19}$$

where $x_2=1-\frac{\lambda}{R}y\tan\psi+\varphi\sin 2\pi(y-t)$, $\varphi=\frac{b}{R}\,(<1)$ is the amplitude ratio, n is the wall-temperature ratio, m is the wall-concentration ratio. Eq. (4) indicates that P is not function of x. Hence P is function of y and t only. In the case of *We* = 0, the Eq. (15) reduces to classical Navier–Stokes equation.

## 3. Method of Solution

Following the studies by El-Sayed *et al.,* [24], we assume solutions for the velocity, temperature and concentration in terms of small perturbation parameters $\varepsilon^2$ in the form

$$\left.\begin{aligned} v&=v_0+\varepsilon^2 v_1+O(\varepsilon^4)\\ T&=T_0+\varepsilon^2 T_1+O(\varepsilon^4)\\ C&=C_0+\varepsilon^2 C_1+O(\varepsilon^4)\end{aligned}\right\}. \tag{20}$$

Substituting Eq. (20) in Eq. (15)-(17) and collecting the coefficient of like powers of $\varepsilon^2$, we get the following set of equations with boundary conditions up to the first order.

The system of the zeroth order is

$$P_y = \frac{\partial}{\partial x}\left[\left(1+We\,\frac{\partial v_0}{\partial x}\right)\frac{\partial v_0}{\partial x}\right] + G_T\,T_0 + G_C\,C_0, \tag{21}$$

$$\frac{\partial^2 T_0}{\partial x^2} = 0, \tag{22}$$

$$\frac{\partial^2 C_0}{\partial x^2} = -Sc\,Sr\,\frac{\partial^2 T_0}{\partial x^2}, \tag{23}$$

and

$$v_0 = 0\ , \quad T_0 = n\ , \quad C_0 = m \qquad at \qquad x = x_1, \tag{24}$$

$$v_0 = 0\ , \quad T_0 = 1\ , \quad C_0 = 1 \qquad at \qquad x = x_2. \tag{25}$$

The system of the first order is

$$0 = \frac{\partial}{\partial x}\left[\left(1+We\,\frac{\partial v_1}{\partial x}\right)\frac{\partial v_1}{\partial x}\right] - v_0 + G_T\,T_1 + G_C\,C_1, \tag{26}$$

$$\frac{\partial^2 T_1}{\partial x^2} = -Ec\,{v_0}^2, \tag{27}$$

$$\frac{\partial^2 C_1}{\partial x^2} = -Sc\,Sr\,\frac{\partial^2 T_1}{\partial x^2}. \tag{28}$$

and

$$v_1 = 0\ , \quad T_1 = 0\ , \quad C_1 = 0 \qquad at \qquad x = x_1. \tag{29}$$

$$v_1 = 0\ , \quad T_1 = 0\ , \quad C_1 = 0 \qquad at \qquad x = x_2, \tag{30}$$

Because, it is not possible to get closed form solutions for Eq. (21)-(23) and (26)-(28) for arbitrary values of all the parameters, we seek the solution of the problem as a power series expansion in the small parameter We as follows

$$\left.\begin{aligned} v_0 &= v_{00} + We\,v_{01} + O(We^2) \\ T_0 &= T_{00} + We\,T_{01} + O(We^2) \\ C_0 &= Cv_{00} + We\,C_{01} + O(We^2) \end{aligned}\right\}. \tag{31}$$

$$\left.\begin{aligned} v_1 &= v_{10} + We\, v_{11} + O(We^2) \\ T_1 &= T_{10} + We\, T_{11} + O(We^2) \\ C_1 &= C_{10} + We\, C_{11} + O(We^2) \end{aligned}\right\}. \tag{32}$$

Substituting from Eq. (31) in Eq. (21)-(23), we obtain the following system of equations

$$P_y = \frac{\partial^2 v_{00}}{\partial x^2} + G_T\, T_{00} + G_C\, C_{00}, \tag{33}$$

$$\frac{\partial^2 T_{00}}{\partial x^2} = 0, \tag{34}$$

$$\frac{\partial^2 C_{00}}{\partial x^2} = -Sc\, Sr \frac{\partial^2 T_{00}}{\partial x^2}, \tag{35}$$

$$0 = \frac{\partial^2 v_{01}}{\partial x^2} + \frac{\partial}{\partial x}\left(\frac{\partial v_{00}}{\partial x}\right)^2 + G_T\, T_{01} + G_C\, C_{01}, \tag{36}$$

$$\frac{\partial^2 T_{01}}{\partial x^2} = 0, \tag{37}$$

$$\frac{\partial^2 C_{01}}{\partial x^2} = -Sc\, Sr \frac{\partial^2 T_{01}}{\partial x^2}, \tag{38}$$

with the boundary conditions

$$v_{00} = 0 \;,\; T_{00} = n \;,\; C_{00} = m \;,\; v_{01} = 0 \;,\; T_{01} = 0 \;,\; C_{01} = 0 \quad at \quad x = x_1, \tag{39}$$

$$v_{00} = 0 \;,\; T_{00} = 1 \;,\; C_{00} = 1 \;,\; v_{01} = 0 \;,\; T_{01} = 0 \;,\; C_{01} = 0 \quad at \quad x = x_2. \tag{40}$$

Solving Eq. (33)-(38) using (39) and (40), yields

$$T_{00} = c_1\, x + c_2, \tag{42}$$

$$C_{00} = c_5\, x + c_6 - Sc\, Sr\, T_{00}, \tag{43}$$

$$v_{01} = c_7\, x + c_8 + \alpha_3\, x^2 + \alpha_4\, x^3 + \alpha_5\, x^4 + \alpha_6\, x^5, \tag{44}$$

$$T_{01} = C_{01} = 0. \tag{45}$$

Substituting from Eq. (32) in Eq. (26)-(28), we obtain the following system of equations

$$0 = \frac{\partial^2 v_{10}}{\partial x^2} - v_{00} + G_T T_{10} + G_C C_{10}, \tag{46}$$

$$\frac{\partial^2 T_{10}}{\partial x^2} = -Ec\, v_{00}{}^2, \tag{47}$$

$$\frac{\partial^2 C_{10}}{\partial x^2} = -Sc\, Sr \frac{\partial^2 T_{10}}{\partial x^2}. \tag{48}$$

$$0 = \frac{\partial^2 v_{11}}{\partial x^2} + \frac{\partial}{\partial x}\left(\frac{\partial v_{10}}{\partial x}\right)^2 - v_{01} + G_T T_{11} + G_C C_{11}, \tag{49}$$

$$\frac{\partial^2 T_{11}}{\partial x^2} = -2Ec\, v_{00}\, v_{01}, \tag{50}$$

$$\frac{\partial^2 C_{11}}{\partial x^2} = -Sc\, Sr \frac{\partial^2 T_{11}}{\partial x^2}. \tag{51}$$

$$v_{10} = 0 \;,\; T_{10} = 0 \;,\; C_{10} = 0 \;,\; v_{11} = 0 \;,\; T_{11} = 0 \;,\; C_{11} = 0 \quad at \quad x = x_1, \tag{52}$$

$$v_{10} = 0 \;,\; T_{10} = 0 \;,\; C_{10} = 0 \;,\; v_{11} = 0 \;,\; T_{11} = 0 \;,\; C_{11} = 0 \quad at \quad x = x_2. \tag{53}$$

The solutions of Eq. (46)-(51) subject the boundary conditions (52) and (53) are given by

$$v_{10} = c_{13}\, x + c_{14} + \alpha_{23}\, x^2 + \alpha_{24}\, x^3 + \alpha_{25}\, x^4 + \alpha_{26}\, x^5 + \alpha_{27}\, x^6 + \alpha_{28}\, x^7 + \alpha_{29}\, x^8 + \alpha_{30}\, x^9 + \alpha_{31}\, x^{10}, \tag{54}$$

$$T_{10} = c_9\, x + c_{10} + \alpha_7\, x^2 + \alpha_8\, x^3 + \alpha_9\, x^4 + \alpha_{10}\, x^5 + \alpha_{11}\, x^6 + \alpha_{12}\, x^7 + \alpha_{13}\, x^8, \tag{55}$$

$$C_{10} = -Sc\, Sr\, T_{10}, \tag{56}$$

$$v_{11} = c_{15}\, x + c_{16} + \alpha_{32}\, x^2 + \alpha_{33}\, x^3 + \alpha_{34}\, x^4 + \alpha_{35}\, x^5 + \alpha_{36}\, x^6 + \alpha_{37}\, x^7 + \alpha_{38}\, x^8 + \alpha_{39}\, x^9 + \alpha_{40}\, x^{10} + \alpha_{41}\, x^{11} + \alpha_{42}\, x^{12} + \alpha_{43}\, x^{13} + \alpha_{44}\, x^{14} + \alpha_{45}\, x^{15} + \alpha_{46}\, x^{16} + \alpha_{47}\, x^{17} + \alpha_{48}\, x^{18} + \alpha_{49}\, x^{19}, \tag{57}$$

$$T_{11} = c_{11}\, x + c_{12} + \alpha_{14}\, x^2 + \alpha_{15}\, x^3 + \alpha_{16}\, x^4 + \alpha_{17}\, x^5 + \alpha_{18}\, x^6 + \alpha_{19}\, x^7 + \alpha_{20}\, x^8 + \alpha_{21}\, x^9 + \alpha_{22}\, x^{10} \tag{58}$$

$$C_{11} = -Sc\, Sr\, T_{11}, \tag{59}$$

All coefficients appearing in the above expressions of solutions are calculated by usual lengthy algebra that involved in regular perturbation method.

Now, the skin friction coefficient $\tau_\omega$, the heat transfer coefficient (Nusselt number) *Nu* and the mass transfer coefficient (Sherwood number) *Sh* at the outer tube, are defined, respectively by

$$\tau_\omega = \left[\left(1+We\right)\frac{\partial v}{\partial x}\right]_{x=x_2}, \qquad Nu = \left.\frac{\partial T}{\partial x}\right|_{x=x_2}, \qquad Sh = \left.\frac{\partial C}{\partial x}\right|_{x=x_2}. \tag{60}$$

The expressions for $\tau_\omega$, *Nu* and *Sh* have been obtained by substituting from Eq. (41)-(45) and (54)-(59) into Eq. (60), and they have been evaluated numerically for several values of the parameters of the problem. The obtained results will be discussed in the next section.

## 4. Results and Discussion

We must choose the porosity parameter and Weisseing number less than one because they have been used as a perturbation parameter. Moreover, the approximation which have been used (long-wavelength approximation) restricted us to choose the values of propagation velocity, wavelength, and radius of the tube such that the wave number is neglected, and Reynolds number is very small. The following values of human small intestine parameters are used as in the previous studies [24, 26, 27].

$y_0$ = 1.25 cm, $c$ = 2 cm/ min, and $\lambda$ = 8.01 cm.

To discuss the effect of various parameters involved in the problem such as Eckert number *Ec*, Grashof number $G_T$, the modified Grashof number $G_C$, the pressure gradient $P_y$, Schmidt number *Sc* and Soret number *Sr*, and Weisseing number *We* on the solution of the considered problem, a numerical results are calculated using Mathematica package 7, for the axial velocity *v*, the temperature distribution *T*, the concentration distribution *C*, the skin friction coefficient $\tau_\omega$, the heat transfer coefficient (Nusselt number) *Nu*, and the mass transfer coefficient (Sherwood number) *Sh* such that $\psi = 8.8, \emptyset = 0.1, \quad y = 0.4, Sr = 1, Sc = 1.5, P_y = 2.5, G_C = 1.5, G_T = 3.5, \varepsilon = 0.22, We = 0.05, Ec = 1, n = 1.25, m = 0.75, \text{and } t = 0.5$

Figure 2 and 3 illustrate the change of the axial velocity *v* versus the radial coordinate y with several values of Ec and Sr, respectively. It is seen, from Figure 2 and 3, that the axial velocity increases with the increase of Ec, whereas it decreases as Sr increases, respectively. It is also noted that the difference of the axial velocity for different values of Ec and Sr becomes greater with increasing the radial coordinate and reaches maximum value after which it decreases. Note that the maximum value of *v* increases by increasing Ec and Sr, and this also occurs at another value x >x0. The effects of $G_T$ and $G_C$ on the axial velocity ware found to be exactly like the effect of Ec given in Figure 2. Similar result to that shown in Figure 2 can be obtained if Ec is replaced by $G_T$ or $G_C$. Also, the behaviour of w with Sc is found to be like the curves in Figure 3, with the only difference that the obtained curves are very close to those obtained in Figure 3.

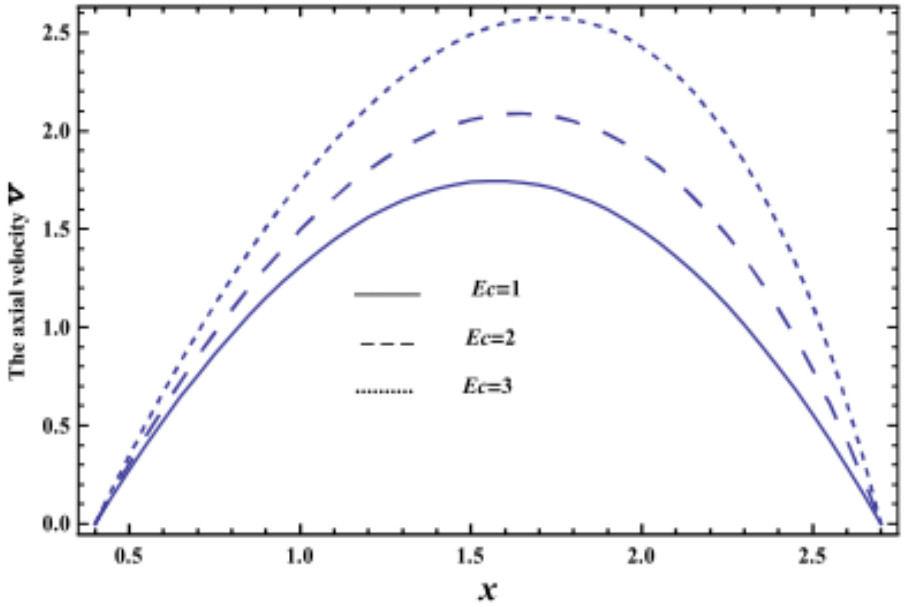


**Fig. 2.** Change of the axial velocity *v* versus the radial coordinate y with several values of Ec

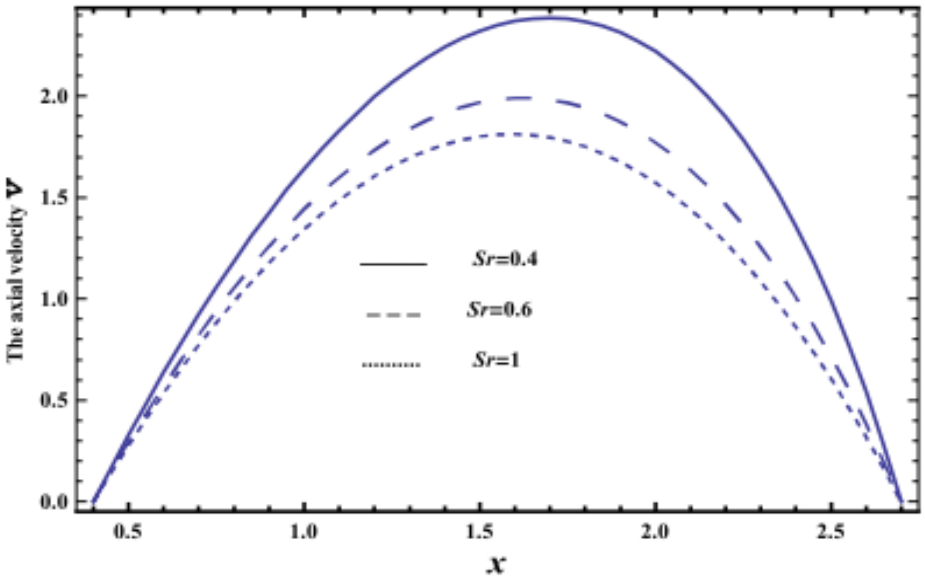


**Fig. 3.** Change of the axial velocity *v* versus the radial coordinate y with several values of Sr

Figure 4 shows the variation of the axial velocity v with x for various values of Weisseing number We, and indicates that for a constant value of We, the axial velocity v increases by increasing x till a maximum value (at a finite value of x: $x = x_0$) after which it decreases. Also, it is found from this figure that the axial velocity v decreases by increasing Weisseing number We when $x \in [0.4, 1.5]$, while it increases afterwards.

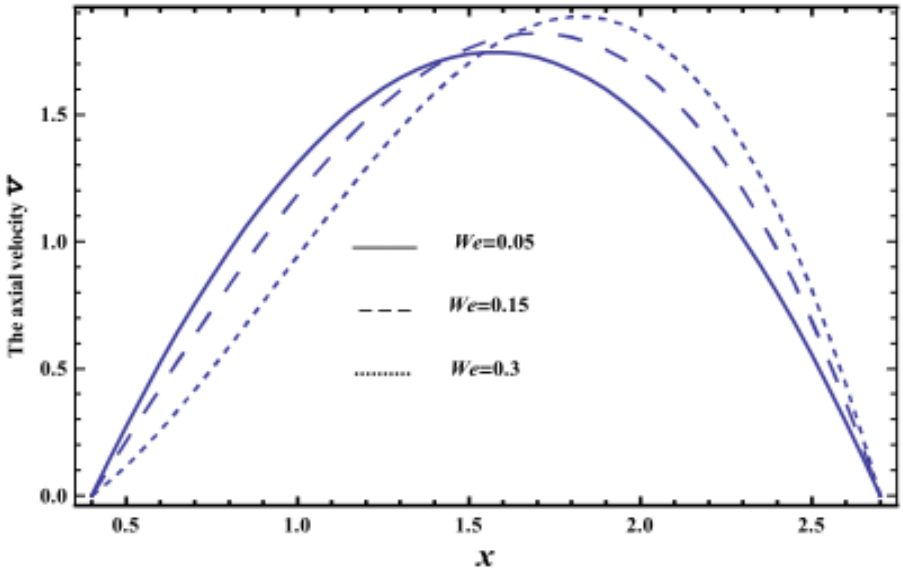


**Fig. 4.** Variation of the axial velocity v with x for various values of Weisseing number, We

The variations of the temperature distribution T with the dimensionless radial coordinate x for various values of Ec and $P_y$, respectively, are displayed in Figure 5 and 6. The graphical results of Figure 5 and 6 indicate that the temperature distribution T increases with increasing in the parameter Ec, while it decreases by increasing the parameter $P_y$, respectively. It is also noted that for small values of Ec and large values of $P_y$, the relation between T and x is approximately linear, and T increases with x till a definite value x=x0 (represents the maximum value of T) and it decreases afterwards. This maximum value of T increases by increasing Ec, while it decreases by increasing $P_y$.

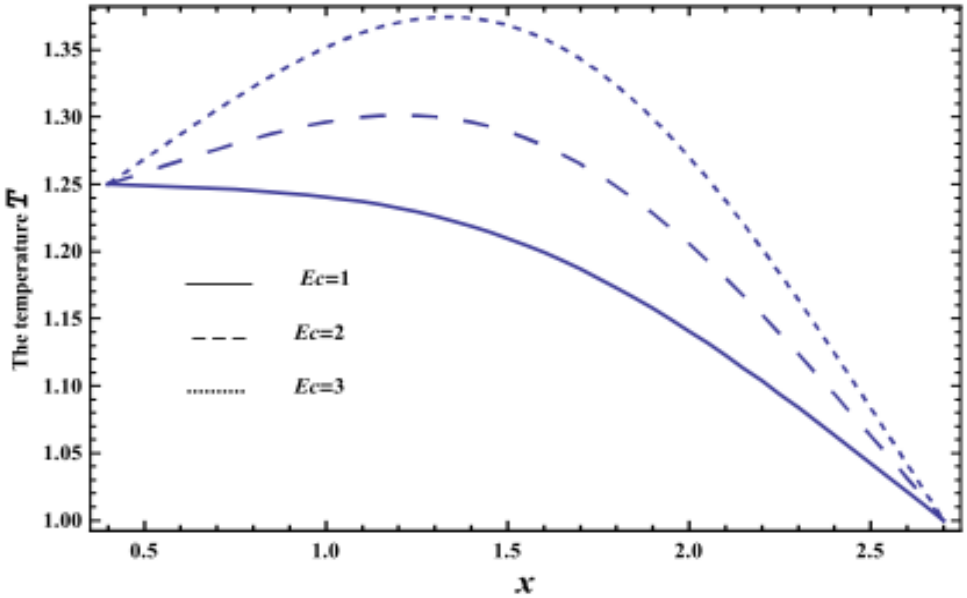


**Fig. 5.** Variations of the temperature distribution T with the dimensionless radial coordinate x for various values of Ec

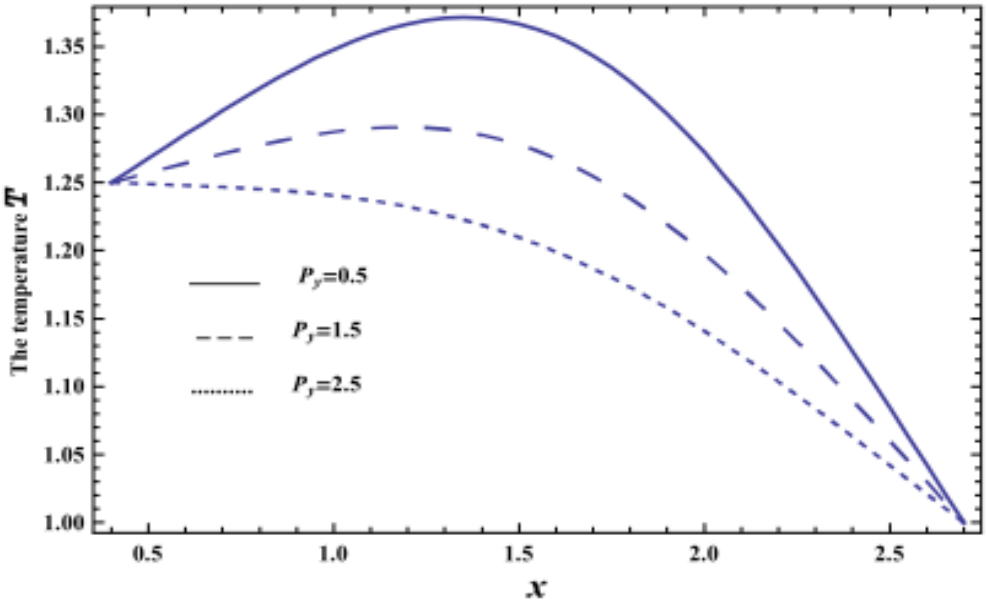


**Fig. 6.** Temperature distribution T with the dimensionless radial coordinate x for various values of $P_y$

The effect of We on the temperature distribution T as a function of the dimensionless radial coordinate x is shown in Figure 7. It is found that the temperature distribution T increases by increasing We in the interval x∈ [0.4, 1.5]; otherwise it decreases by increasing We. So, the behavior of T in the interval x∈ [0.4, 1.5], is an inversed manner of its behavior in the interval x∈ [1.5, 2.7] except that the curves are very close to each other in the second interval. In this case, for small values of We, there is a maximum value of T holds at x =0.4.

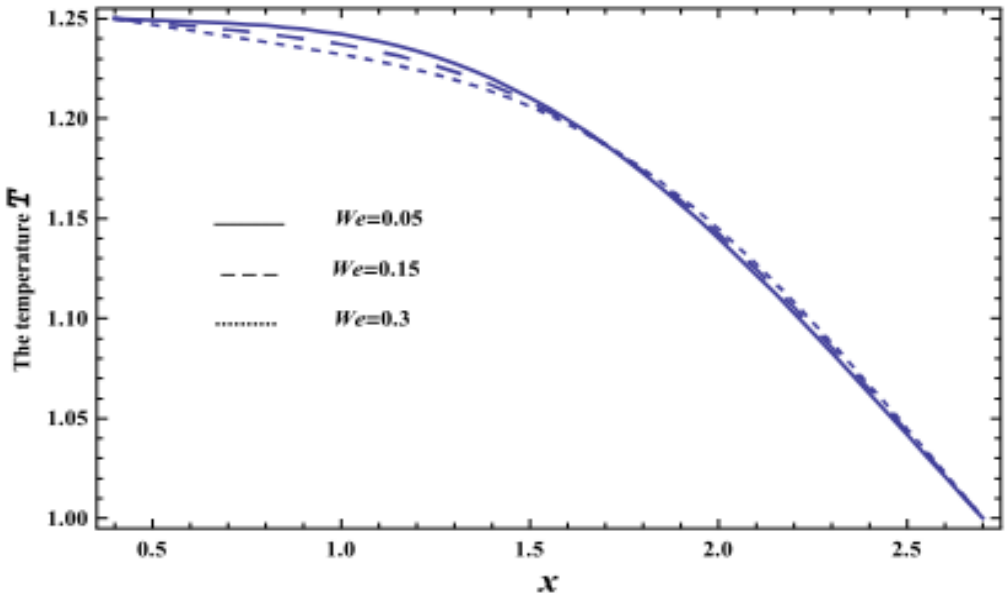


**Fig. 7.** Temperature distribution T as a function of the dimensionless radial coordinate x

Figure 8 and 9 represent the behaviours of the concentration distribution C with the dimensionless radial coordinate x for different values of Ec and $P_y$, respectively. It is observed from Figure 8 and 9, that the concentration distribution C decreases with the increase of Ec, whereas it

increases as $P_y$ increases, respectively. It is also noted that the difference of the concentration distribution C for different values of Ec and $P_y$ becomes greater with increasing the radial coordinate x and reaches minimum value, after which it increases. Figure 10 illustrates the effect of We on the concentration distribution C as a function of the dimensionless radial coordinate x. It is found that in the interval of the radial coordinate x∈ [0.4, 1.5], the behavior of C for various values of We is exactly similar to the behavior of C for various values of $P_y$ given in Figure 9. It is also noted, from Figure 10 that in the interval of the radial coordinate x∈ [0.4, 1.5], the behavior of C is an inversed manner of its behavior in the interval x∈ [1.5, 2.7] except that the curves are very close to each other in the second interval. In this case, for any value of the parameter We, there is a minimum value of C holds at x =1.2, and this minimal slightly decreases by increasing the value of We.

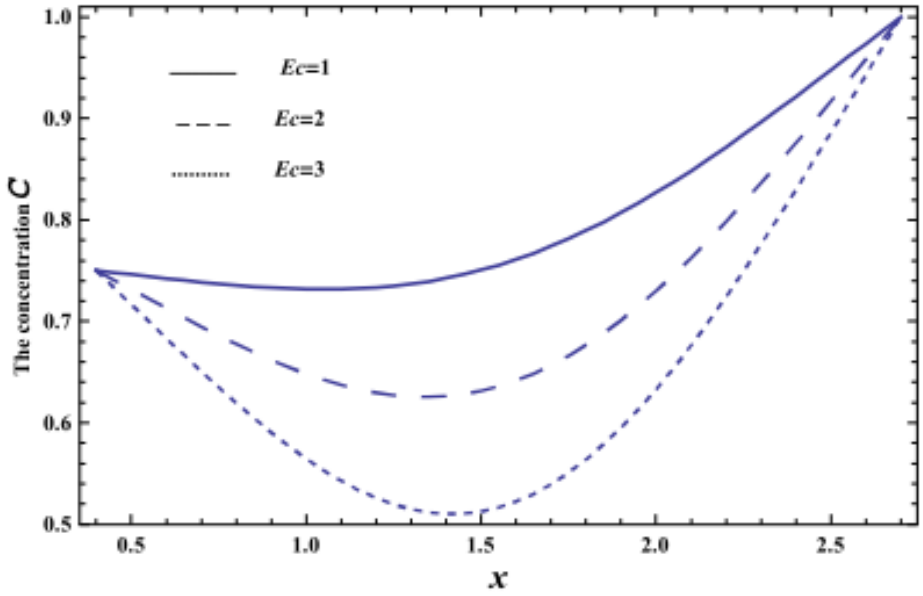


**Fig. 8.** Behaviours of the concentration distribution C with the dimensionless radial coordinate x for different values of Ec

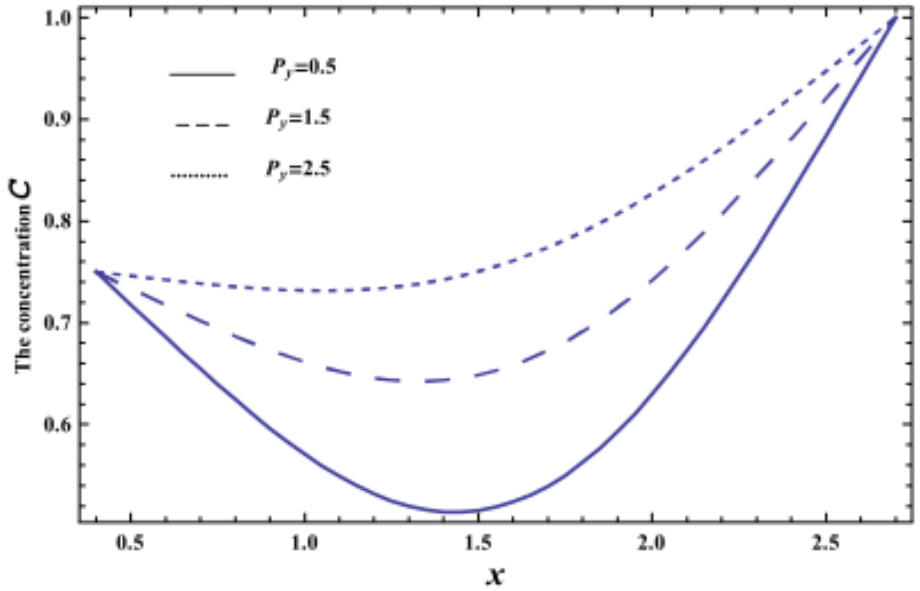


**Fig. 9.** Behaviours of the concentration distribution C with the dimensionless radial coordinate x for different values of $P_y$

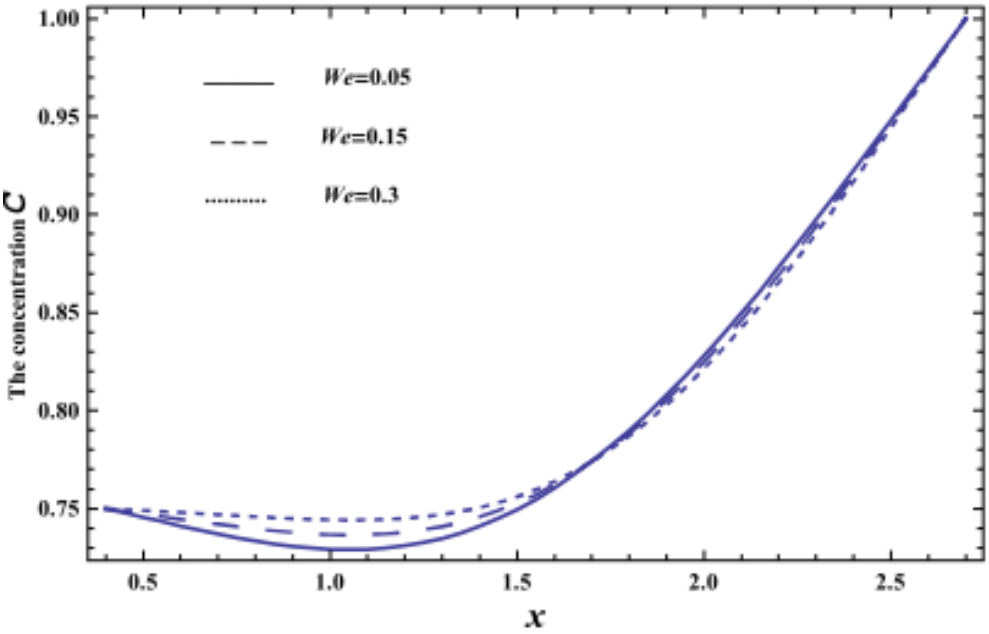


**Fig. 10.** Effect of We on the concentration distribution C as a function of the dimensionless radial coordinate x

The skin-friction distribution$\tau\omega$ within the axial coordinate y∈[0, 1] are exhibited in Figure 11 and 12, for various values of Sr and Ec, respectively. From these figures, it is observed that the skin-friction$\tau\omega$ increases with the increase of Sr, whereas it decreases as Ec increases, respectively. It is also noted that for each value of both Sr and Ec, $\tau\omega$ is always negative, and all obtained curves are coinciding in the wide part of the tube y∈[0, 0.4], after which $\tau\omega$ decreases as y increases. The effects of the other parameters are found to be similar to them; these figures are excluded here to avoid any kind of repetition.

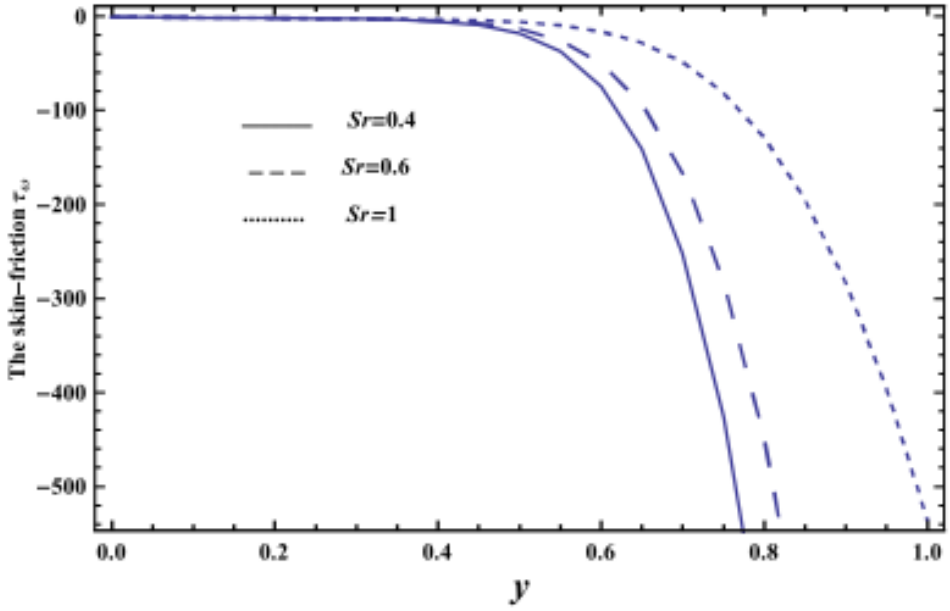


**Fig. 11.** Skin-friction distribution$\tau\omega$ within the axial coordinate y∈[0, 1] for various values of Sr

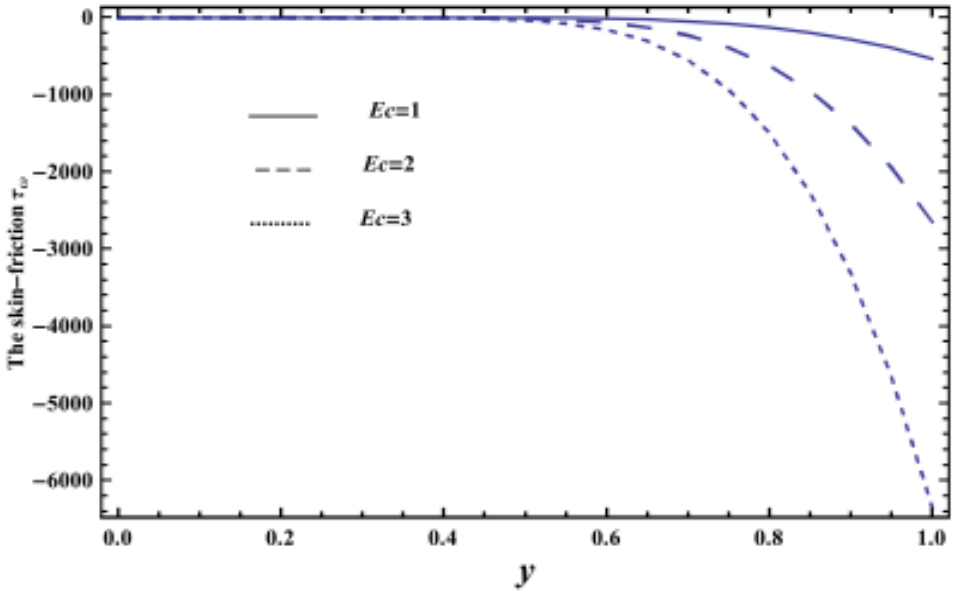


**Fig. 12.** Skin-friction distribution$\tau\omega$ within the axial coordinate y∈[0, 1] for various values of Ec

Figure 13 and 14 show the behaviours of Nusselt number Nu with the axial coordinate y, for various values of $P_y$ and $G_T$ respectively. It is noted from Figure 13 that the resulting in this case will be like those obtained in Figure 11 for the effect of Sr on $\tau\omega$ except that Nu increases as y increases till its maximum value after which it decreases. Also, Figure 14 shows that the effect of $G_T$ on Nu is like the effect of Ec on $\tau_\omega$ given by Figure 12, except that for small values of $G_T$, there is a linear relation between Nu and y. The effects of $G_C$ and We on Nu (figures are removed) are found to be exactly like the effect of $G_T$ on Nu given in Figure 14, with the only difference that the obtained curves are very close to those obtained in Figure 14.

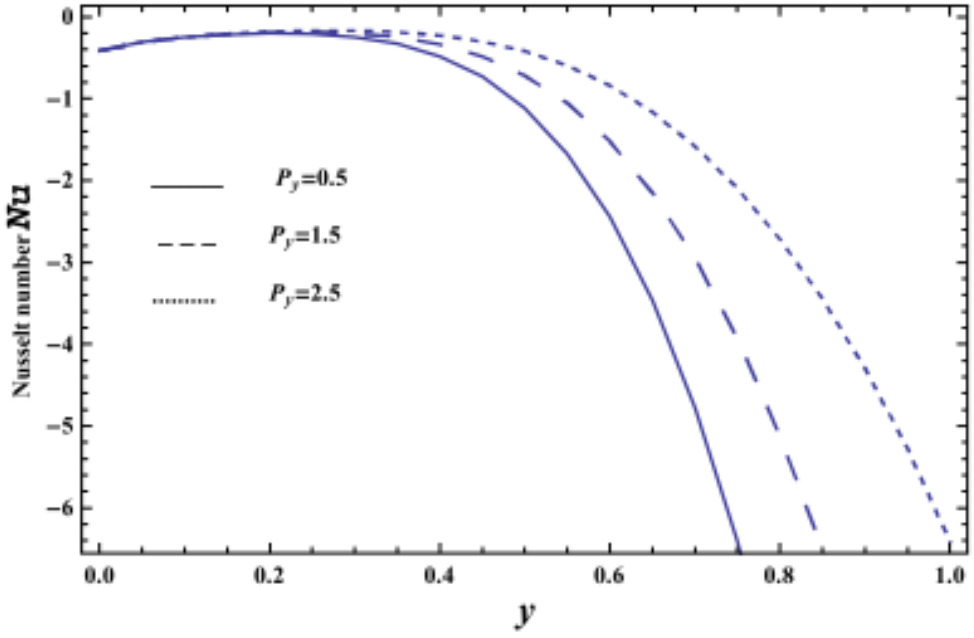


**Fig. 13.** Behaviours of Nusselt number Nu with the axial coordinate y, for various values of $P_y$

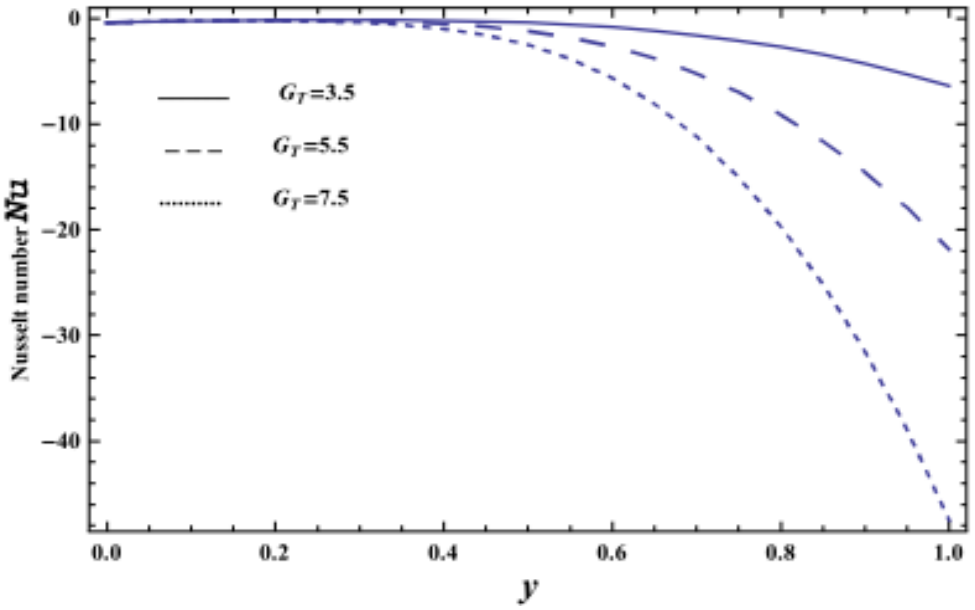


**Fig. 14.** behaviours of Nusselt number Nu with the axial coordinate y, for various values of $G_T$

Figure 15 and 16 illustrate the effects of $G_C$ and $P_y$ on Sherwood number Sh with the axial coordinate y, respectively. It is clear from these figures that Sh decreases as y increases till a minimum value, after which Sh increases and all obtained curves are coincide in the wide part of the tube, namely y∈[0, 0.25]. Also, the effect of $P_y$ is to decrease Sherwood number, whereas it increases as $G_C$ increases. The effects of the parameters Ec, $G_T$ and We on Sh (figures are excluded) are found to be like the effect of $G_C$ on Sh given in Figure 15.

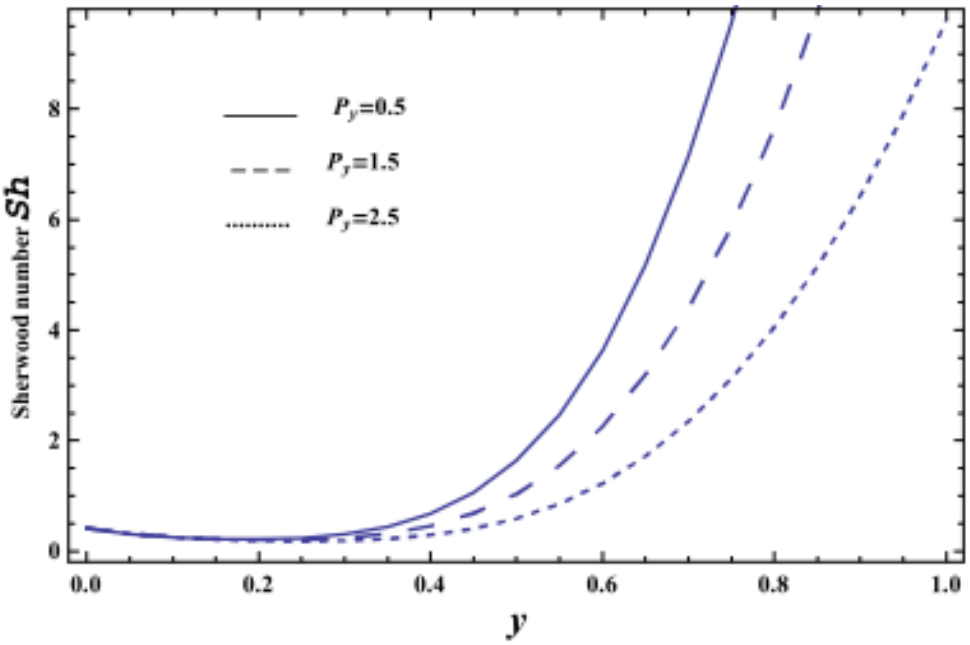


**Fig. 15.** Effects of $P_y$ on Sherwood number Sh with the axial coordinate y

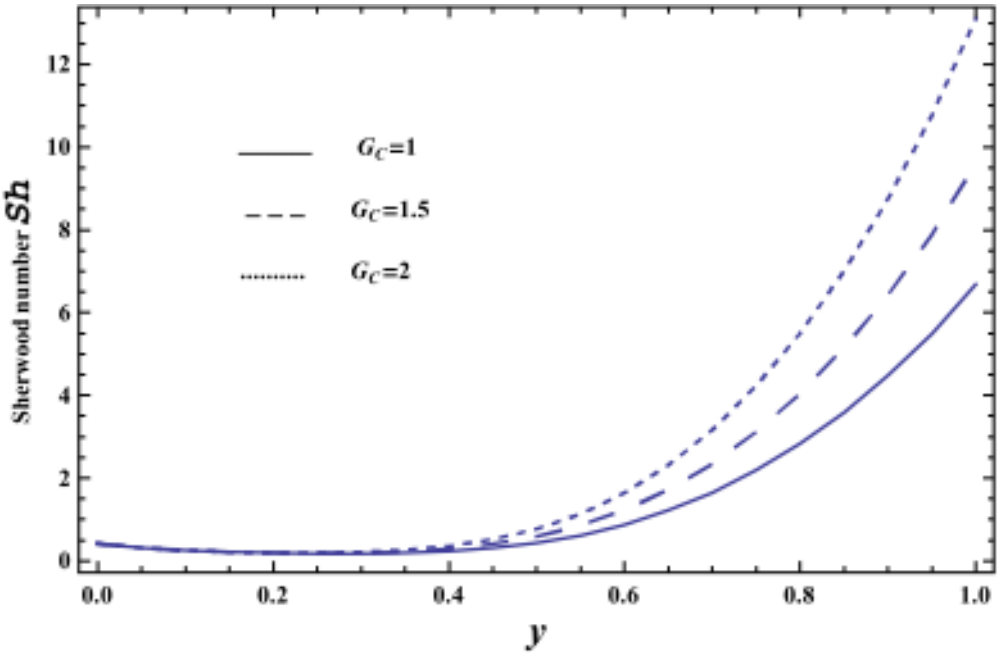


**Fig. 16.** Effects of $G_C$ on Sherwood number Sh with the axial coordinate y

## 5. Conclusion

In this article, peristaltic flow of an incompressible Williamson fluid through vertical porous medium in the gap between two co-axial tubes with heat and mass transfer has been studied for the long wavelength at low Reynolds number. The outer tube is non-uniform and has a sinusoidal wave traveling down its wall, while the inner one is a rigid, and uniform. We studied the problem in 2D case using the cartesian coordinates, because it is well known that the long-wavelength asymptotic approximation in 3D case is not as good as in 2D case and the 3D flow is more sensitive to Reynolds number change [24, 27]. The present analysis can serve as a model which may help in understanding the mechanics of physiological flows[28, 29]. The expressions for the velocity, temperature, concentration distributions as well as the skin friction, Nussselt number and Sherwood number at the wavy wall of the outer tube have been discussed graphically. The following observations have been found.

i. The axial velocity v increases or (decreases) with the increase in Weissenberg number We.
ii. The axial velocity v increases with the increase each of Ec, GT and GC, whereas it decreases as Sc and Sr increase.
iii. The axial velocity v for different values of all parameters becomes greater with increasing the radial coordinate x and reaches maximum value (at a finite value of x: x = x0) after which it decreases.
iv. The temperature increases with the increase each of Ec, GT and GC, and We whereas it decreases as $P_y$ increases.
v. The concentration has an opposite behavior compared to temperature behavior except that it decreases with the increase of both Sr and Sc, while all the obtained lines of temperature will coincide.
vi. By increasing each of Ec, GT and GC, the skin-friction distribution $\tau\omega$ decreases, while it increases as Sc and Sr increase.
vii. By increasing each of GT and GC, Nusselt number Nu decreases, while it increases as $P_y$ increases.

viii. Sherwood number Sh has an opposite behaviour compared to Nusselt number Nu.

ix. For any values of $0.4 \leq y \leq 1$, Nu and Sh decrease, while for any values of $0 \leq y \leq 0.4$, all the obtained lines will coincide.

## References

[1] Fung, Y.C. and Yih, Y.C. "Peristaltic transport." *Journal of Applied Mechanics* 35, no. 4 (1968): 669-675.
[2] Burns, J.C. and Parkers, T. "Peristaltic motion." *Journal of Fluid Mechanics* 29, (1970): 731-743.
[3] El Naby, Abd El Hakeem Abd, and A. E. M. El Misiery. "Effects of an endoscope and generalized Newtonian fluid on peristaltic motion." *Applied Mathematics and computation* 128, no. 1 (2002): 19-35.
[4] Rathod, V. P., and M. M. Channakote. "A study of ureteral peristalsis in cylindrical tube through porous medium." *Advances in Applied Science Research* 2, no. 3 (2011): 134-140.
[5] Divya B., Manjunatha G., Rajashekhar C., Hanumesh V. and Kerehalli V. P. " Influence of velocity and thermal slip on the peristaltic transport of a herschel-bulkley fluid through an inclined porous tube." *Journal of Advanced Research in Fluid Mechanics and Thermal Sciences* 56, no. 2 (2019): 195-210.
[6] Gudekote, Manjunatha, and Rajashekhar Choudhari. "Slip effects on peristaltic transport of Casson fluid in an inclined elastic tube with porous walls." *Journal of Advanced Research in Fluid Mechanics and Thermal Sciences* 43, no. 1 (2018): 67-80.
[7] Abou-zeid, Mohamed, Abeer A. Shaaban, and Muneer Y. Alnour. "Numerical treatment and global error estimation of natural convective effects on gliding motion of bacteria on a power-law nanoslime through a non-Darcy porous medium." *Journal of Porous Media* 18, no. 11 (2015): 1091-1106.
[8] Elshahed, Moustafa, and Mohamed H. Haroun. "Peristaltic transport of Johnson-Segalman fluid under effect of a magnetic field." *Mathematical Problems in Engineering* 2005, no. 6 (2005): 663-677.
[9] Abou-zeid, Mohamed Y., and Mona AA Mohamed. "Homotopy perturbation method for creeping flow of non-Newtonian power-law nanofluid in a nonuniform inclined channel with peristalsis." *Zeitschrift für Naturforschung A* 72, no. 10 (2017): 899-907.
[10] Hayat, T., and N. Ali. "On mechanism of peristaltic flows for power-law fluids." *Physica A: Statistical Mechanics and Its Applications* 371, no. 2 (2006): 188-194.
[11] Choudhari, Rajashekhar, Manjunatha Gudekote, Hanumesh Vaidya, and Kerehalli Vinayaka Prasad. "Peristaltic flow of Herschel-Bulkley fluid in an elastic tube with slip at porous walls." *Journal of Advanced Research in Fluid Mechanics and Thermal Sciences* 52, no. 1 (2018): 63-75.
[12] Nadeem, S., and Noreen Sher Akbar. "Effects of heat and mass transfer peristaltic flow of Williamson fluid in a vertical annulus." *Meccanica* 47, no. 1 (2012): 141-151.
[13] Abou-Zeid, Mohamed. "Effects of thermal-diffusion and viscous dissipation on peristaltic flow of micropolar non-Newtonian nanofluid: application of homotopy perturbation method." *Results in Physics* 6 (2016): 481-495.
[14] Eldabe, Nabil, and Mohamed Abou-Zeid. " Radially varying magnetic field effect on peristaltic motion with heat and mass transfer of a non-Newtonian fluid between two co-axial tubes." *Thermal Science* 22, no. 6 (2018): 2449-2458.
[15] Abou-Zeid, Mohamed Y. "Homotopy perturbation method for couple stresses effect on MHD peristaltic flow of a non-Newtonian nanofluid." *Microsystem Technologies* 24, no. 12 (2018): 4839-4846.
[16] Abou-Zeid, M. Y. "Homotopy perturbation method to gliding motion of bacteria on a layer of power-law nanoslime with heat transfer." *Journal of Computational and Theoretical Nanoscience* 12, no. 10 (2015): 3605-3614.
[17] Beng, Soo Weng, and Wan Mohd Arif Aziz Japar. "Numerical analysis of heat and fluid flow in microchannel heat sink with triangular cavities." *Journal of Advanced research in fluid mechanics and thermal sciences* 34 (2017): 1-8.
[18] Vajravelu, K., S. Sreenadh, P. Devaki, and K. V. Prasad. "Peristaltic transport of a Herschel–Bulkley fluid in an elastic tube." *Heat Transfer—Asian Research* 44, no. 7 (2015): 585-598.
[19] Chaturani, P., and S. Narasimman. "Theory for flow of Casson and Herschel-Bulkley fluids in cone-plate viscometers." *Biorheology* 25, no. 1-2 (1988): 199-207.
[20] Shaaban, Abeer A., and Mohamed Y. Abou-Zeid. "Effects of heat and mass transfer on MHD peristaltic flow of a non-Newtonian fluid through a porous medium between two coaxial cylinders." *Mathematical Problems in Engineering* 2013 (2013): 1-11.
[21] Eldabe, N. T., and M. Y. Abou-Zeid. "The wall properties effect on peristaltic transport of micropolar non-Newtonian fluid with heat and mass transfer." *Mathematical Problems in Engineering* 2010 (2010): 1-40.
[22] Afifi, N. A. S. "Study of peristaltic flow for different cases." PhD diss., Ph. D. Thesis, Ain Shams University, Cairo, Egypt, 1998.
[23] Elshehawey, Elsayed F., Ayman MF Sobh, and Elsayed ME Elbarbary. "Peristaltic motion of a generalized Newtonian fluid through a porous medium." *Journal of the Physical Society of Japan* 69, no. 2 (2000): 401-407.

[24] El-Sayed, M. F., N. T. M. Eldabe, A. Y. Ghaly, and H. M. Sayed. "Effects of chemical reaction, heat, and mass transfer on non-Newtonian fluid flow through porous medium in a vertical peristaltic tube." *Transport in porous media* 89, (2011): 185-212.
[25] Hayat, T., N. Ali, and S. Asghar. "Hall effects on peristaltic flow of a Maxwell fluid in a porous medium." *Physics Letters A* 363, no. 5-6 (2007): 397-403.
[26] El-Dabe, Nabil, Abeer A. Shaaban, Mohamed Y. Abou-Zeid, and Hemat A. Ali. "Magnetohydrodynamic non-Newtonian nanofluid flow over a stretching sheet through a non-Darcy porous medium with radiation and chemical reaction." *Journal of Computational and Theoretical Nanoscience* 12, no. 12 (2015): 5363-5371.
[27] Abou-zeid, Mohamed. "Magnetohydrodynamic boundary layer heat transfer to a stretching sheet including viscous dissipation and internal heat generation in a porous medium." *Journal of Porous Media* 14, no. 11 (2011): 1007-1018.
[28] El-dabe, Nabil TM, Mohamed Y. Abou-zeid, and Yasmeen M. Younis. "Magnetohydrodynamic peristaltic flow of Jeffry nanofluid with heat transfer through a porous medium in a vertical tube." *Applied Mathematics & Information Sciences*11, no. 4 (2017): 1097-1103.
[29] Abdull Yamin, E. S., and Che Sidik N. A. "Prediction of Fluid Flow in Artificial Cancellous Bone." *Journal of Advanced Research in Materials Science* 3, no. 1 (2014): 8-14.